Induced phase modulation of chirped continuum pulses studied with a femtosecond frequency-domain interferometer

E. Tokunaga and A. Terasaki

Department of Physics, Faculty of Science, University of Tokyo, 7-3-1 Hongo, Bunkyo, Tokyo 113, Japan

T. Kobayashi*

Frontier Research Program, RIKEN, The Institute of Physical and Chemical Research, 2-1 Hirosawa, Wako, Saitama 351-01, Japan

Received October 14, 1992

The effect of rapid phase change on chirped continuum pulses is studied with a frequency-domain interferometer. Because of the chirp, temporal evolution of the optical Kerr response in CS_2 is projected into difference phase spectra. The chirped continuum shows spectral shifts that are due to induced phase modulation even when the continuum has a flat spectrum.

When a femtosecond white-light continuum pulse is used in femtosecond spectroscopy, the frequency chirp, which is caused by positive group-velocity dispersion of optical elements,[1] must be phase compensated to obtain true transient spectra, otherwise the spectra will have a wavelength-dependent time-delay distortion. Because of higher-order phase distortion, however, it is difficult to eliminate the relative phase difference completely over the whole spectral range of the continuum even with a combination of negative group-velocity dispersion optical configurations.[2] Instead, delay time correction in the transient spectra is often performed. In this case, however, it is not obvious if it gives us equivalent results to those observed with a chirp-compensated pulse.

In this Letter the effect of rapid phase change on a chirped continuum is studied to show that there is a residual effect of the chirp that cannot be eliminated even after delay time correction. For this purpose, the phase change of the continuum induced by the optical Kerr response of a transparent Kerr liquid CS_2 is measured with a frequency-domain interferometer.[3]

The laser source, amplification, and measurement systems were described in a previous Letter.[3] The amplified pulses of 60-fs duration, 620-nm wavelength, 10-kHz repetition rate, and 2-μJ energy are divided into the pump and probe pulses. The probe is focused into an ethylene glycol jet to generate a white-light continuum. The continuum pulse is further divided into the two arms of a Michelson interferometer for the reference and probe, and the two pulses are displaced temporally by a few hundreds of femtoseconds. Then they travel along a common path and are detected by a spectrometer with a multichannel photodiode array after being transmitted through a sample. The pump is blocked by a mechanical shutter at 10 Hz to obtain difference spectra with and without excitation.

Typical results of CS_2 in a 1-mm cell are shown in Fig. 1. The excitation density was approximately 5.7×10^{-3} J/cm^2. Figure 1(a) shows probe spectra with and without excitation and the difference transmission spectra (DTS), which were taken by blocking the reference beam. Figure 1(b) shows normalized interference spectra with and without excitation and the difference phase spectra (DPS; open circles). The DPS were derived by the same procedure as before.[3]

Figure 2 displays the DTS and DPS without delay time correction at three time delays, where zero delay is defined at the maximum overlap between the pump and probe at 620 nm. Since the continuum is positively chirped after passing through optical elements of ~11-mm total thickness, the red region of the probe arrives earlier at the sample than does

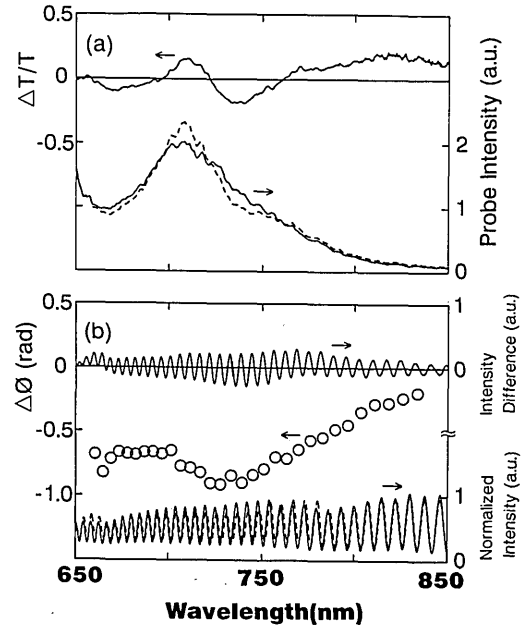

Fig. 1. Signals for CS_2 without delay-time correction. (a) DTS (upper solid curve) and probe spectra with excitation (dashed curve) and without excitation (lower solid curve) by the pump–probe measurement. (b) DPS (open circles), interference spectra with (dashed curve) and without (lower solid curve) excitation, and the difference interference spectrum between them (upper solid curve). Here the interference is normalized by the probe spectrum without excitation.

0146-9592/93/050370-03$5.00/0

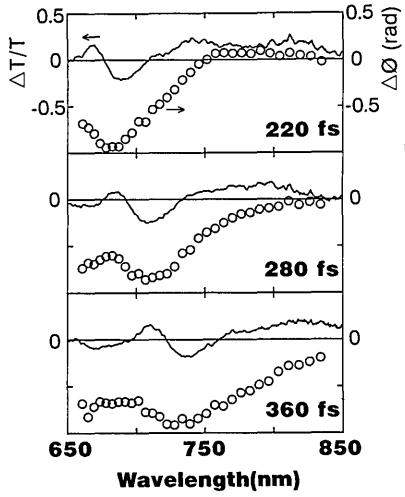

Fig. 2. DTS and DPS in CS_2 obtained by chirped continuum pulses at 220-, 280-, and 360-fs time delays without delay-time correction. Zero delay is defined at the maximum overlap between the pump and probe at 620 nm.

the blue region such that the decrease in wavelength corresponds to the increase in time delay. Hence, the DPS do not rise instantaneously over the whole spectral range but show a characteristic shape that reflects the temporal evolution of the Kerr response in CS_2: the instantaneous electronic response and the subsequent nuclear response[4] with decreasing wavelength. That is, because of the one-to-one correspondence between frequency and time in the chirped continuum, the temporal Kerr dynamics is projected into the frequency domain.

Note also that the DTS are not zero but show an appreciable oscillatory structure. When the time delay is increased from 220 to 360 fs, the DPS signal moves toward a longer wavelength. The oscillatory structure also moves following the DPS, so that the DTS and DPS signals should be closely related to each other. In order to clarify the origin of the DTS signals, a numerical calculation is performed to simulate the experimental results. For this purpose, the frequency chirp of the continuum must be well characterized.[5] To estimate the chirp, the time delay was plotted against the peak wavelength of the DPS as shown in Fig. 3 (circles). Here we used the peak of the DTS instead of that of the DPS because the wavelengths of both peaks coincide with each other. This gives a much easier method for measuring the chirp than does the conventional cross-correlation method.[6] The solid curve is a fitting function: $\tau(\nu) = a + b\nu^2 + c\nu^4$ with $a = 1090$, $b = -3540$, and $c = -4460$. Here τ is the time delay in femtoseconds and ν is the frequency in petahertz (10^{15} Hz).

If the probe-pulse field is assumed to have linear chirp, the probe field is expressed by

$$E(\omega - \omega_0) = E_0(\omega - \omega_0)\exp[-i\rho(\omega - \omega_0)^2], \quad (1)$$

where ρ is a linear chirp parameter. If $E_0(\omega) = E_0\pi^{1/2}\exp(-\tau_p{}^2\omega^2/4)$, where τ_p is the $1/e$ half-width of the probe-field envelope, inverse Fourier transform of Eq. (1) leads to the temporal dependence of the pulse field:

$$E(t) = F^{-1}[E(\omega - \omega_0)]$$
$$= E_0(\epsilon - i\gamma)^{1/2}\exp[i\omega_0 t - (\epsilon - i\gamma)t^2],$$

where $\epsilon = \tau_p{}^2/(\tau_p{}^4 + 16\rho^2)$ and $\gamma = 4\rho/(\tau_p{}^4 + 16\rho^2)$. If $\tau_p{}^2 \ll 4\rho$, $\gamma \sim 1/(4\rho)$. Since $\Phi(t) = \omega_0 t + \gamma t^2$, the instantaneous frequency is $\omega = \mathrm{d}\Phi/\mathrm{d}t = \omega_0 + 2\gamma t$. Therefore ρ is obtained from the slope of a t–ν curve as $\rho \sim (1/2)\mathrm{d}t/\mathrm{d}\omega = -(1/2)\mathrm{d}\tau/\mathrm{d}\omega$. From the fitting function, $\rho = 350$ fs^2 at 700 nm.

The simulation is performed as follows:

$$F[E(t)] = R(\omega)\exp[i\Phi(\omega)],$$
$$F\{E(t)\exp[i\Delta\Phi(t - \tau)]\} = R(\omega, \tau)\exp[i\Phi(\omega, \tau)],$$
$$\Delta T/T(\omega, \tau) = [R^2(\omega, \tau) - R^2(\omega)]/R^2(\omega),$$
$$\Delta\Phi(\omega, \tau) = \Phi(\omega, \tau) - \Phi(\omega),$$

where $E(t)$ is the inverse Fourier transform of the probe-pulse field [Eq. (1)] with $\rho = 350$ fs^2 and a hyperbolic-secant envelope $E_0(\omega)$. According to the probe spectra in Fig. 1(a), $|E(t)|^2$ is assumed to have a 6-fs FWHM in the Fourier-transform limit ($\rho = 0$). $\Delta\Phi(t)$ is a phase change that consists of the electronic and nuclear response terms, where the former is assumed to be the same as the pump-pulse intensity function with 60-fs FWHM and the latter is assumed to be the same function as Eq. (3) in Ref. 4. The results are shown in Fig. 4, which reproduces the observed spectral shifts fairly well. It is therefore proved that the DTS signals are caused by induced phase modulation[7]; rise and decay in the DPS with decreasing wavelength, i.e., with increasing time delay, are accompanied by red and blue shifts of the probe frequency, respectively.

The DTS signals can also be explained as follows. Suppose the probe pulse experiences a small phase change $\Delta\Phi(t)$, which follows a Gaussian pump-intensity profile with a $1/e$ half-width of τ_e such that

$$\Delta\Phi(t) = \delta\exp(-t^2/\tau_e{}^2), \qquad \delta \ll 1,$$
$$E(t)\exp[i\Delta\Phi(t)] \sim E(t)[1 + i\delta\exp(-t^2/\tau_e{}^2)]. \quad (2)$$

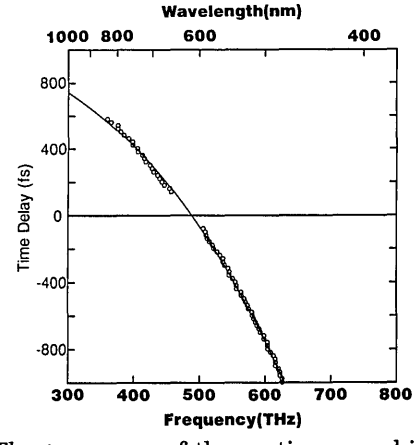

Fig. 3. The t–ν curve of the continuum, which was obtained from the results in Fig. 2 by plotting the time delays against the wavelengths at the peaks of the DTS. The solid curve is the fitting function (see text).

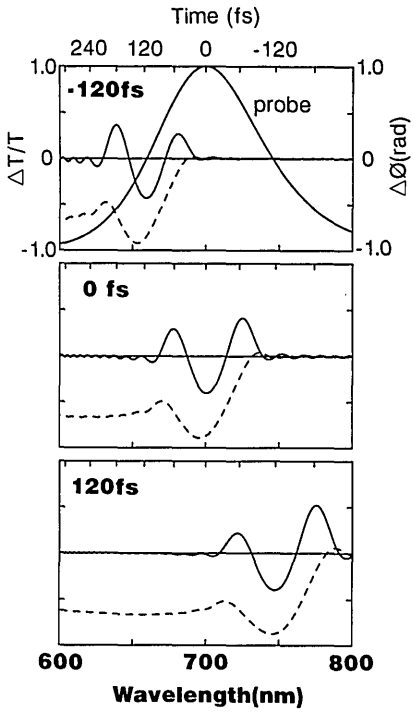

Fig. 4. Results of the simulation (see text). The probe spectrum and the DTS (solid curve) and DPS (dashed curve) are shown at −120-, 0-, 120-fs time delays. The calibrated time is scaled on the top horizontal line.

The Fourier transform of the right-hand side of relations (2) is

$$F[E(t) + iE(t)\Delta\Phi(t)] = E(\omega) + i\delta E_{ex}(\omega),$$

$$E_{ex}(\omega) = \frac{E_0\pi^{1/2}(\epsilon - i\gamma)^{1/2}}{(1/\tau_e^2 + \epsilon - i\gamma)^{1/2}} \exp\left[\frac{-\omega^2}{4(1/\tau_e^2 + \epsilon - i\gamma)}\right].$$

The DTS is expressed as

$$\begin{aligned}\Delta T/T(\omega) &= |[E(\omega) + i\delta\, E_{ex}(\omega)]/E(\omega)|^2 - 1 \\ &\sim -2\delta\ \mathrm{Im}[E_{ex}(\omega)/E(\omega)] \\ &= -2\delta\ \mathrm{Im}((\epsilon - i\gamma)^{1/2}/(1/\tau_e^2 + \epsilon - i\gamma)^{1/2} \\ &\quad \times \exp\{-\omega^2/[4(1/\tau_e^2 + \epsilon - i\gamma)] \\ &\quad + \tau_p^2\omega^2/4 + i\rho\omega^2\}).\end{aligned}$$

In the limit of a broad probe spectrum ($\tau_p \to 0$),

$$\begin{aligned}\Delta T/T(\omega) \sim -2\delta\ \mathrm{Im}((-i\gamma)^{1/2}/(1/\tau_e^2 - i\gamma)^{1/2} \\ \times \exp\{-\omega^2/[4(1/\tau_e^2 - i\gamma)] + i\rho\omega^2\}).\end{aligned} \quad (3)$$

Further, when ρ is much larger than τ_e^2 [$\gamma = 1/(4\rho) \ll 1/\tau_e^2$] and $\rho > 0$,

$$\begin{aligned}\Delta T/T \sim \delta(1/2\rho)^{1/2}\tau_e \exp(-\tau_e^2\omega^2/4) \\ \times (\cos\rho\omega^2 - \sin\rho\omega^2).\end{aligned} \quad (4)$$

The oscillation observed in the DTS can be explained qualitatively by relation (4), although the condition $\gamma \ll 1/\tau_e^2$ is not satisfied in the present experiment because $\rho = 350$ fs^2 and $\tau_e = 43$ fs.

It should be noted that frequency shifts due to induced phase modulation are observed even when the probe spectrum is flat; the shifts depend not only on the spectral shape but also on the chirp. When the continuum has a flat spectrum ($\tau_p = 0$) and is not chirped ($\rho = 0$), no signal is observed in DTS ($\Delta T/T = 0$), as readily derived from relation (3). This is because all the frequency components of the probe have the largest amplitude at the same time such that the frequency shift of any component is canceled by the shift of its neighboring components. When the continuum is chirped, on the other hand, the frequency and time are related linearly through $\Delta\omega = 2\gamma\Delta t$ such that the frequency shift of one component interferes with its neighboring components to give frequency-domain interference as in relation (4).

Even after delay time correction is performed for the signals in Fig. 2, the spectral shifts observed in the DTS cannot be eliminated, so that the corrected spectra will not show the intrinsic dynamics. The DTS and DPS free from the probe-pulse modulation effect can be obtained only with a probe pulse with a flat spectrum and without chirp, i.e., a δ-function pulse in the time domain. In femtosecond spectroscopy, therefore, it is essential to use a continuum with as small chirp as possible. In the real measurements, however, the chirp cannot be eliminated completely, so that the original chirp of a continuum should always be taken into account when interpreting the corrected spectra.

This research was carried out at the Frontier Research Program, RIKEN, with the support of A. F. Garito, A. Yamada, H. Sasabe, and T. Wada. We express our sincere thanks to them for their support during this research.

*Permanent address, Department of Physics, Faculty of Science, University of Tokyo, 7-3-1 Hongo, Bunkyo, Tokyo 113, Japan.

References

1. Z. Bor and B. Racz, Appl. Opt. **24,** 3440 (1985), and references therein.
2. R. L. Fork, C. H. Brito Cruz, P. C. Becker, and C. V. Shank, Opt. Lett. **12,** 483 (1987).
3. E. Tokunaga, A. Terasaki, and T. Kobayashi, Opt. Lett. **17,** 1131 (1992).
4. T. Hattori and T. Kobayashi, J. Chem. Phys. **94,** 3332 (1991).
5. See, for example, J.-C. Diels, J. J. Fontaine, I. C. McMichael, and F. Simoni, Appl. Opt. **24,** 1270 (1985); J. E. Rothenberg and D. Grischkowsky, J. Opt. Soc. Am. B **2,** 626 (1985); K. Naganuma, K. Mogi, and H. Yamada, IEEE J. Quantum Electron. **25,** 1225 (1989).
6. R. L. Fork, C. V. Shank, C. Hirlimann, R. Yen, and W. J. Tomlinson, Opt. Lett. **8,** 1 (1983).
7. See, for example, R. R. Alfano and P. P. Ho, IEEE J. Quantum Electron. **24,** 351 (1988); T. Hattori, A. Terasaki, T. Kobayashi, T. Wada, A. Yamada, and H. Sasabe, J. Chem. Phys. **95,** 937 (1991).